

Development of Fully Noninductive Scenario at High Bootstrap Current Fraction for Steady State Tokamak Operation on EAST

B. Wan¹, A.M. Garofalo², X. Gong¹, J. Li¹, C.T. Holcomb³, W.M. Solomon⁴, A.W. Hyatt², G.L. Jackson², J.R. Ferron², C.C. Petty², S. Ding¹, J. Qian¹, Y. Sun¹, G. Xu¹, G. Li¹, Q. Ren¹, W. Guo¹ and C. Pan¹

¹*Institute of Plasma Physics, Chinese Academy of Sciences, Hefei, China*

²*General Atomics, P.O. Box 85608, San Diego, California 92186-5608, USA*

³*Lawrence Livermore National Laboratory, 7000 East Ave, Livermore, CA 94550, USA*

⁴*Princeton Plasma Physics Laboratory, PO Box 451, Princeton, NJ 08543-0451, USA*

EAST is a fully superconducting tokamak with ITER-like divertor configurations and heating schemes. EAST has achieved and extended H-mode plasma for a duration of over 30s [1]. In order to further extend higher performance plasma to steady-state with reactor relevant boundary conditions, EAST has undergone significant upgrades, including heating and current drive power of over 20MW, RMP coils, and the top tungsten divertor. In parallel, joint experiments were performed, aimed at developing and understanding a steady-state scenario on DIII-D that could be extended to long pulse on EAST. The chosen approach is based on a previously developed high β_P scenario, which is fully non-inductive and characterized by high β_N and an ITB with high bootstrap current fraction $f_{BS} \geq 80\%$ [2]. Such a plasma regime is desirable for steady-state tokamak operation since it reduces the demands on external current drive. The new experiments exploited new DIII-D capabilities to test such a steady-state scenario under EAST relevant conditions, including more off-axis external current drive, low NBI torque, and low I_p ramping rate. The approach for fully non-inductive operation is to remove the current drive from the transformer via clamping the OH coils.

Figure 1 shows temporal evolution of several plasma parameters for a typical discharge. The plasma cross section is an upper biased double-null divertor shape, with elongation $\kappa \sim 1.86$ and average triangularity (top and bottom) $\delta \sim 0.6$. The toroidal field is $B_T = 2.0$ T. After an approximate stationary condition is established (1.7 s), the current in the transformer coil is clamped, so that the plasma current is forced to relax non-inductively. A flattop at $I_p \sim 0.6$ MA is maintained by increasing β_N and thus the bootstrap current fraction, until a 100% non-inductive condition is achieved and maintained for the rest of the discharge up to heating limitation. The discharge was achieved and maintained at $\beta_N \sim \beta_P \geq 3$ and $\beta_T \sim 1.5\%$ using a total heating and current drive power of ~ 11 MW including ~ 5 MW of off-axis NBI ($\rho \sim 0.4$), and 2.5 MW of off axis electron cyclotron current drive (ECCD) ($\rho \sim 0.5$). The various current components plotted in Fig. 1(a) are calculated with TRANSP from kinetic equilibrium using

experimental profiles. The bootstrap current fraction reaches 80%–85%, the NBI-driven current fraction is 15%–20%, and ECCD <5% of the total current.

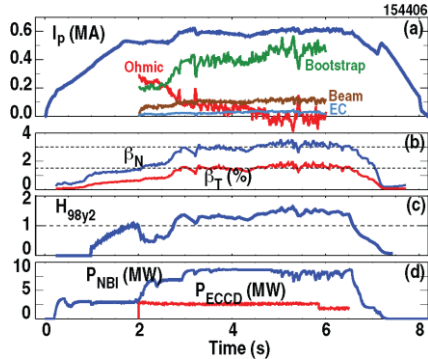


Fig. 1. A fully non-inductive regime. The OH coils are clamped after 1.7 s. (a) Plasma current and its various components, (b) β_N (blue), and β_T (red), (c) H_{98y2} , factor and (d) injected heating and current drive power, (e) Equilibrium reconstruction at 5.0s, almost up–down symmetric.

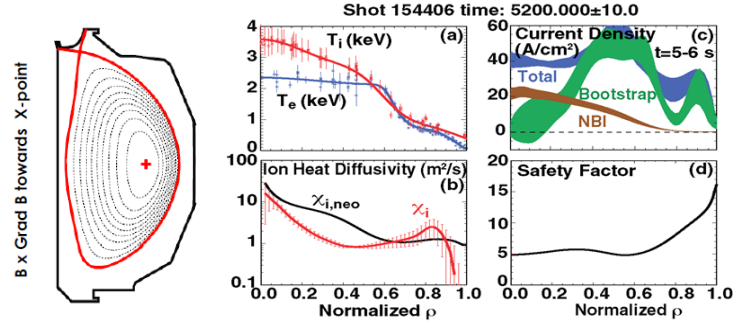


Fig. 2. Radial profiles for discharge 154406 in Fig. 1 at $t=5.2$ s. (a) T_e and T_i , (b) ion heat diffusivity, compared to the neoclassical value, (c) current density profiles for the total current and its main components, and (d) safety factor.

Excellent confinement is achieved, and is associated with the formation of an ITB at large minor radius in all channels (n_e , T_e , T_i). Figure 2(a) shows representative radial profiles for T_e and T_i , both exhibiting a large gradient at $\rho \sim 0.7$. The ion heat diffusivity is dropped to the neoclassical inside of $\rho < 0.7$ as shown in Fig. 2(b), indicating minimal turbulent transport driving ion thermal transport. A very broad bootstrap current profile shown in Fig. 2(c) is fairly well-aligned with the total current profile, explaining why q_{min} is high [Fig. 2(d)]. The ITB is maintained for ~ 4 s, longer than three times the current relaxation time τ_{CR} , which is estimated to be ~ 1 s. These data support that the ITB observed at $\rho \sim 0.7$ can be consistent with steady-state operation.

EAST has two NBI beam lines in the balanced injection configuration, providing maximum toroidal torque of $\sim \pm 3$ Nm. An important question is whether the above non-inductive high bootstrap fraction regime can be achieved with lower NBI torque on EAST. New experiments reproduced excellent confinement similar to that achieved in 2004 experiments (~ 7 Nm) [2], but with the lower NBI torque expected on EAST (~ 3 Nm) shown in Fig. 3, although counter NBI reduced NBCD slightly. The profiles of ion temperature and toroidal rotation are shown in Fig. 4 for two shots with different NBI torques, where 5Nm for #154380 and 3Nm for #154383. Two shots have similar density and electron temperature and their profiles. The center rotations in both cases are similar, but having broader profile in the core region with higher NBI torque and out half radial region with lower NBI torque. Correspondingly, ion temperature profiles are similar to rotation, which leads to similar plasma performance for these two shots. Preliminary linear analysis using GYRO shows that

high rotation may suppress the growth of linear mode (ITG/KBM), but $E \times B$ shear (stabilization) and rotation shear (destabilization) compete with each other.

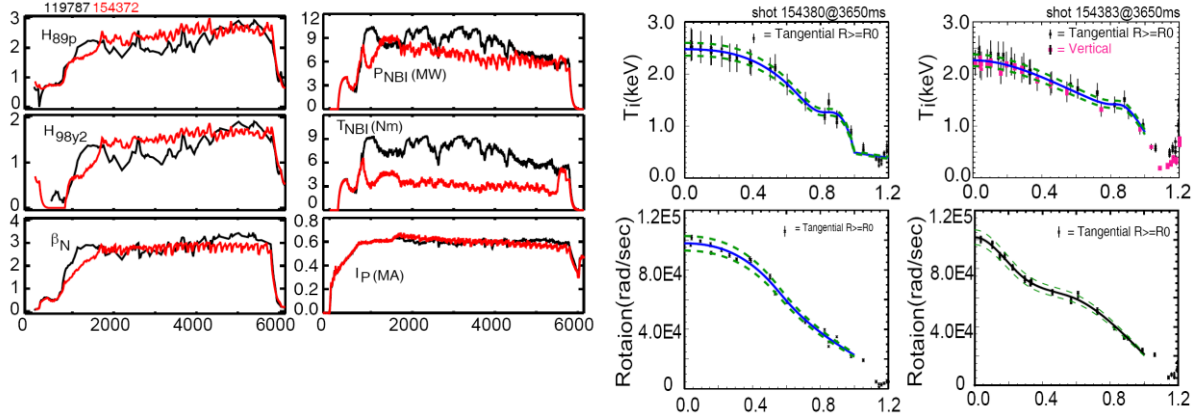


Fig. 3. A shot (154372, red) with lower NBI torque compared with previous non-inductive high poloidal beta discharge (ref [2])

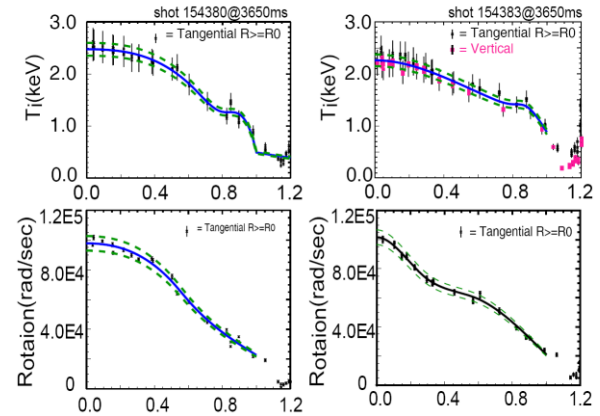


Fig. 4. Toroidal and ion temperature profiles for two shot with different NBI torques. Left: 5Nm for #154380 , right 3Nm for #154383

A broad current profile with high q_{min} is obtained at low plasma current ramp-up rate of 0.25MA/s, comparable to the limits of the superconducting PF coils on EAST, by reducing the initial gas injection rate. Despite the different current ramping rate, discharges reached steady-state with similar confinement and normalized beta, as shown in Fig. 5, where $dI_p/dt \sim 0.7$ MA/s for #154374 and 0.25MA/s for #154392. To reach the stationary state at low dI_p/dt is obviously lagged compared to higher dI_p/dt . It is however not an issue for long pulse operation on EAST if such a regime has been established within the PF limitation.

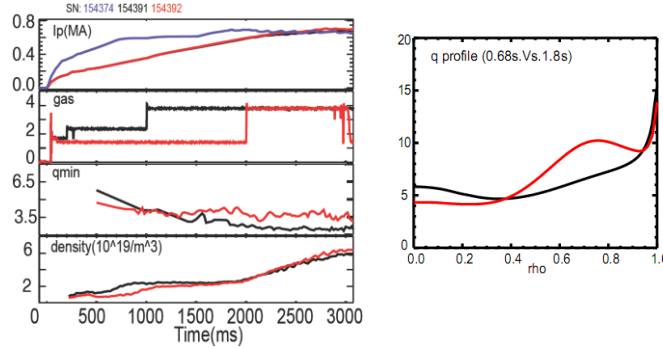


Fig. 5. Use a current ramp-up rate consistent with EAST constraints: ~ 0.25 MA/s, validated early H&CD required by future superconducting tokamak. High q_{min} with slower I_p ramp-up maintained with reduction of early gas injection.

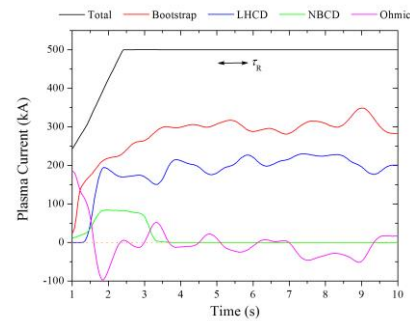


Fig. 6. Prediction for steady-state operation with fully non-inductive scenario. The major parameters are listed in table 1(S_1)

A further important result, providing evidence of dynamical stability, is that the ITB partially collapses with the large ELMs at enough high beta particularly at the highest obtained $\beta_N \sim 3.5$, but it quickly recovers. Stability analysis shows that this β_N value is very close to the MHD stability limit with an ideal wall. ELM dynamics appear as a limiting instability toward stationary sustainment of even higher performance. These fully

non-inductive high bootstrap discharges need to pursue integration of ELM control on both EAST and DIII-D. On DIII-D, reducing the early gas injection has led to onset of an Edge Harmonic Oscillation, suggesting that the ELM-stable regime of QH-mode may be accessible. On EAST, LHCD has been found to drive a small but significant helical current in the boundary plasma [3], which leads to a three-dimensional distortion of magnetic topology at the edge, mitigating the ELMs in a wide range of q_{95} . Additional, mitigation of ELMs also has been demonstrated in EAST with multi-pulses of Supersonic Molecular Beam Injection. Future experiments will test methods of ELM control to enable a further increase of β_N and thus of I_P and β_T . It should be noted, however, that the levels of normalized fusion performance already achieved and sustained fully non-inductively ($\beta_T \sim 1.5\%$, $f_{BS} \sim 85\%$, and $f_G \sim 90\%$), may be sufficient for economic electricity generation in a steady-state fusion reactor using available technology.

Table 1. Zero-dimensional estimation and 1.5D simulation show that EAST with half available powers can challenge steady-state operation at $I_p=0.5$ MA with fully non-inductive current drive.

	I_p (MA)	B_i (T)	β_N	n_e/n_G	H_{98y2}	$li(1)$	f_{BS}	f_{CD}	P_{NB} (MW)	P_{IC} (MW)	P_{LH} (MW)
S_1	0.5	2.5	2.35	0.7	1.2	0.9	0.6	0.4	4	6	2.8
S_2	0.5	2.5	2.7	0.7	1.17	0.88	0.6	0.4	4	9	2.6

Simulations using PTRANSP with the multi-mode transport model show that the high β_p scenario demonstrated on DIII-D is accessible on EAST for 0.5MA steady-state plasma at $\beta_N \sim 2.35$ (2.7) and with bootstrap current fraction of 60% (60%) by utilizing half of the total H&CD capabilities planned for 2014 (Table 1). NBI is used only during the plasma current ramp up phase for pre-heating. High performance plasma is fully sustained by ICRF and LHW power (Fig. 5). A weak core magnetic shear similar to the DIII-D scenario and with ITB footprint at $\rho \sim 0.6$ is achieved in the simulations. The scenario demonstrated on DIII-D and predicted for EAST could be extended to durations for many times the current relaxation time and even the wall equilibration time using the expected EAST capabilities in the upcoming campaign. Success of this endeavor will be a significant progress toward the goal of fusion energy.

This work was supported in part by the US Department of Energy under DE-FC02-04ER54698, DE-AC52-07N27344, and DE-AC02-09CH11466, and the National Magnetic Confinement Fusion Science Program of China under No. 2011GB101000.

Reference

- [1] B.N. Wan, et al., Nucl. Fusion 53 (2013) 104006
- [2] P.A. Politzer, et al., Nucl. Fusion 45, 417 (20052).
- [3] J. Li, et al., Nature Phys. 9, 817 (2013).